Indian Journal of Fundamental and Applied Life Sciences ISSN: 2231– 6345 (Online)
An Open Access, Online International Journal Available at www.cibtech.org/sp.ed/jls/2015/02/jls.htm
2015 Vol. 5 (S2), pp. 2714-2729/Loveymi and Barati
Research Article

OBTAINING COMPRESSIVE FLOW CURVE OF AZ41 MAGNESIUM ALLOY REINFORCED BY 0.3 PERCENT SILICON AT HIGH TEMPERATURE AND VARIOUS STRAIN RATES

***Ali Loveymi and Farzan Barati**
Department of Mechanics, Science and Research Branch, Islamic Azad University, Hamedan, Iran
**Author for Correspondence*

ABSTRACT
In this paper, obtaining the curve of compressive flow stress of AZ41 magnesium with0.3% silicon additive at high temperatures and different strain rates has been considered. Also, according to this issue that the frictional behavior of a material is used in the production processes, especially the forming processes, frictional behavior of this alloy at different deformation temperatures has been analyzed. Compression T-shape test has been examined. The compression tests of AZ60 magnesium alloy have been carried out at temperatures of 230 and 250°C and under the loading rates of $0.001s^{-1}$, $0.01s^{-1}$, and $0.1s^{-1}$. Initial stress value with bending correction factor has been calculated and then using finite element simulation with DEFORM software and multistep correction, the numerical correction factors were obtained for each temperature and certain strain rate. The results show that, in stress-strain curves of AZ60alloy at low strains, the stress values calculated from numerical correction factor and bending correction factor are slightly different. But with increasing the strain, the difference between the stresses calculated from numerical correction factor is greater than bending correction factor and always the calculated stress is higher than bending correction factor. Also, the bending correction factor at all temperatures has increased with increasing of the strain. At a constant temperature, with increasing strain rate the maximum stress of the material is increased and at constant strain rates by increasing temperature, the maximum stress is reduced.

Keywords: *Magnesium Alloys, Compression Test, Correction Factor, Friction, T-Shape Test, Temperature, Strain Rate*

INTRODUCTION
Today magnesium alloys are of interest to many researchers and have been widely used in major industries including car manufacturing and aerospace industries (Cáceres, 2009). In addition to light weight, there are other desired characteristics in magnesium alloys such as appropriate strength that make these alloys distinguished for other metals to be used in different industries. Some of these properties are the ratio of strength to high weight, good fricative strength, welding capability, and recycling capability (Cáceres, 2009). Wang *et al.*, (2011) studied the effect of adding Bi to microstructures and mechanical properties AZ80 magnesium alloy. The results showed that with addition of Bi, hard eutectic phases are improved and become non-continuous. Also, when the amount of Bi is greater than 1%, the amount of initial layer of Mg3 Bi2 phase increases, which splits the bed and the tensile strength and elongation reduce. Wu *et al.*, (2009) studied the microstructures and mechanical properties of AZ31B magnesium alloy recycled by solid-state process from different size chips. Recycled specimens showed lower ductility than reference ones; also, recycled samples with average surface area of the chips have the highest elongation. Grain size, the amount of oxide, and density of ingot were effective in elongation of recycled materials Chen *et al.*, (2011) investigated the mechanical properties and microstructures of AZ60D magnesium alloy provided by compound extrusion. Strength and ductility of the alloy significantly improved after treatment for grain and uniform distribution between the metal particles. In addition, the hardness of AZ41D alloy significantly increased with increasing strain from 0 to 8.240.With increasing strain rate, the hardness slightly increases.
Aghayanni *et al.*, (2011) investigated the effects of ultrasound on the microstructure and tensile strength of AZ60 magnesium alloy. The results showed that ultrasonic treatment of molten material before milling

has a significant effect on the size and being spherical the α-mg dendrites, as well as the size, continuity, and the distribution between the metal particles formed during cooling and the strength of the alloy. Liao *et al.*, (2011) studied the effect of thermo-electro pulsing rolling on mechanical properties and microstructure of AZ31 magnesium alloy. The results showed that WR reduces the rate of elongation compared to raw specimen, while the TER increased this parameter. Saniei *et al.*, (2013) studied the behavior of compressive stress and tensile stress of AZ80 magnesium alloy. The previous pressure test should be performed at zero friction conditions, but it is impossible to provide such conditions. Therefore, increasing correction factor and numerical correction factor are used to eliminate the effect of friction between the surfaces. Tensile tests were carried out on standard samples at high temperatures and different strain rates. The effect of necking phenomena was corrected using Bridgeman correction factor and was simulated using finite element software. Also, the density T-test was used to evaluate the parameter of friction at high temperatures. Saniei *et al.*, (2012) studied an exponential model to predict the flow curves of several groups of AZ magnesium alloys in tension and pressure. This paper is about flow behavior of various magnesium alloys in tension and pressure such as AZ31, AZ80, and AZ81.The tests were done at elevated temperatures and high strain rates. To eliminate the effect of heterogeneous deformation in tension and pressure tests, the numerical method and Bridgeman method were used. A two-part mathematical model was used to predict the curves of flow stress of different magnesium alloys in various tension and pressure. In addition, based on the proposed model, the stress was estimated at peak state. The actual stress and strain of the necking point were estimated using a similar relationship. Also, the behavior of the estimated flow was compatible with experimental results. Kim *et al.*, (2010) studied a strategy for creating ultrafine-grained microstructure in magnesium alloy sheets. Li *et al.*, (2013) investigated the effect of solution heat treatments on microstructure and hardness of ZK60 magnesium alloys prepared under low-frequency alternating magnetic fields. Results show that comparing with observed microstructure in the non-detection of electromagnetic field the eutectic network structure is better found at grain boundaries under the low-frequency alternating magnetic fields and is displayed as uniform grain distribution. Caton *et al.*, (2002) and Mathis *et al.*, (2002) studied the deformation behavior of AZ41, AS21 and AE42 magnesium commercial alloys at a wide range of temperature and different strain rates. To detect the hardening and softening, they investigated and calculated the correlation of stress to hardness strain factor. They also carried out experiments at temperatures of 20 to 300ºC and strain rates of 0.0001^{s1} and showed that hardening decreases with increasing temperature and stress. Masoudpanah and Mahmoudi (2010) studied the tensile and shear deformations and microstructure of AZ31 alloy after extrusion and ECAP. The ECAP samples comparing with extruded samples had lower yield stress and higher tensile ductility. Zhao *et al.*, (2010) studied in similar conditions the mechanical tensile properties and microstructure of ZK60-Y alloys that have been produced by two different ways. Easton *et al.*, (2010) compared deformations of magnesium alloys with aluminum and steel alloys in terms of tension, bending, and buckling. Results showed that magnesium alloys compared to mild steel had higher energy absorption and strength in bending and buckling. Anbuselvan *et al.*, (2010) investigated deformation of Z60 A magnesium alloy using a pressure test. The temperature range of the pressure test has been 300 to 500°C. Their research showed that the temperature and strain rate are important in shaping the magnesium alloy. Furthermore, the optimal parameters in forming AZ60 magnesium alloy are the temperature of 400°C and strain rate of 0.001^{s1}. Sung *et al.*, (2010) studied the strain rate sensitivity of the cast magnesium alloys. They examined the behavior of three alloys of AM20, AM50 and AM60 in a wide range of strain rate, from strain rate of $0.001s^{-1}$ to $1700s^{-1}$.Theresults showed that in low strain rates, the sensitivity to strain rate reduces with increase in amount of aluminum alloy element in magnesium alloy. In addition, at strain rates higher than $1500s^{-1}$, the rate of hardness strain and strain rate sensitivity and as a result, the flow stress of the material will greatly increase.

Many studies have been done on the stress-strain relations between magnesium alloys and alloys that have similar behaviors with these alloys, especially at high temperatures, and some models have been proposed to predict their behaviors. Ebrahimi *et al.*, (2006) proposed a mathematical model to show the

stress-strain curves of Ti-IF steel alloys at elevated temperatures. The results of their model are in good agreement with empirical results. Zhou *et al.*, (1990) investigated the workability of AZ80 magnesium alloy. They studied the compressive tests at temperature range of 200 to 500°C and strain rates of$0.001s^{-1}$to $20s^{-1}$.

Due to friction between the contact surfaces in the pressure test, the sample becomes barreling. Several research have been done to eliminate the effect of friction at stress-strain curve and also on barreling deformation of the specimens. Ettouney and Stelson (1983) carried out researches one deformation of the specimen during pressure test at room temperature. They proposed a model to determine the rate of deformation in different strains and used it to determine the friction. Narayanasamy *et al.*, (2000) performed a study on barreling deformation of magnesium alloys. The results showed that the radius of the barreling of the specimen has a linear relationship with geometric factor. Saniei *et al.*, (2006) carried out a research on pressure test and correction of strain-stress curves. Using numeral simulations, they provided a numeral correction factor that comparing to bending correction factor has better agreement with empirical results. Bending correction factor is entirely geometrical and in which the effects of other parameters effective in deformation process are not considered. By numerical simulation of process and considering the effect of friction, they provided numerical correction factor. Bending correction factor always increases with increasing strain, while the numerical correction factor reduces in high strains and with increasing the effect of friction in the process. To investigate the accuracy of their results, they carried out the empirical tests on specimens fabricated of tin and lead at room temperature. They also studied the effect of dimensional ratio, hardening strain exponent and strength factor in numerical correction factor.

In the present study, obtaining a compressive flow stress curve of AZ41 magnesium with0.3% silicon additive at high temperatures and different strain rates is investigated.

In previous studies, the effect of the friction factor, the ratio of height to diameter of the sample, strength factor and the rate of hardness strain on numerical correction factor were investigated (Saniei and Fatehi, 2006).

In that study, the samples made of lead and tin were used to perform pressure testing at room temperature. Also, the experiments were performed at a constant strain rate, and strain rate sensitivity has been assumed to be negligible. Magnesium alloys are sensitive to strain rate and forming them is done at high temperatures.

Therefore, pressure tests were conducted at two temperatures and three strain rate. Thus, investigation of effect of strain rate and temperature in correction factor are important. So, the effects of strain rate and temperature in correction factors were studied. The modeling of stress-strain curves of AZ60 magnesium alloys at different temperatures and strain rates is studied.

Tests to Determine the Friction Factor and Stress-strain Curve

Investigation of the Effects of Parameters with Numerical Simulations

To estimate force sensitivity to friction, the sensitivity of curve slope is defined as following:

$$\lambda_k = \frac{K_m - K_{m=0}}{K_{m=0}} \qquad (1)$$

Where, K_m is the curve slope of the force with friction factor of m, and $K_{m=0}$is the curve slope of the force in condition that m=0 (conditions without friction).

Pressure Test

In this experiment, compressors with flat plates compress a cylindrical sample. The diameter changes of each step are recorded. The following relations are valid for uniform compression test.

$$\bar{\varepsilon} = \ln\frac{h_o}{h} = \ln\frac{A}{A_o} \qquad (2)$$

$$\bar{\sigma} = \frac{P}{A} \qquad (3)$$

Where, A_o and A are the moment and initial section areas, h and h_o are the moment and initial heights and $\bar{\varepsilon}$ and $\bar{\sigma}$ are effective strain and effective stress respectively and P is the force exerted on the specimen.

The Method of Bending Correction Factor

In the bending correction factor method, the flow stress of material is determined using stress analysis of middle section of a pressurized cylindrical sample between two parallel plates. The analysis assumed that the materials are homogeneous, isotropic, and incompressible. Considering the balance condition in the radial direction r and using geometrical conditions and plasticity equations, the following equations are obtained using mathematical calculations (Mielnik, 1990):

$$\sigma_r = \bar{\sigma}\ \ln\left(\frac{a^2 - 2aR - r^2}{-2aR}\right) = -\bar{\sigma}\ \ln\left(\frac{2aR}{2aR - a^2 + r^2}\right) \quad (4)$$

$$\sigma_z = \bar{\sigma}\ [1 + \ln\left(\frac{a^2 - 2aR - r^2}{-2aR}\right)] = \bar{\sigma}[1 + \ln\left(\frac{2aR}{2aR - a^2 + r^2}\right)] \quad (5)$$

Where, $\bar{\sigma}$ is the effective stress of the material, and in Von Mayors criterion, it is calculated from following equation:

$$\bar{\sigma} = \frac{1}{\sqrt{2}}[(\sigma_z - \sigma_r)^2 + (\sigma_r - \sigma_\theta)^2 + (\sigma_z - \sigma_\theta)^2]^{1/2} \quad (6)$$

In the above equations, the different parameters are as following:

σ_θ, σ_z and σ_r the principal stresses in the peripheral and axial and radial directions respectively, and a is middle section radius of the specimen, r is the radius of the location of the desired element and R is the radius of curvature of the barrel lateral side of the sample. Compressive force P at each section of the sample is given by the following equation:

$$P = O_0^a\ S_z\ 2\text{prdr} = pa^2(S_Z)_{\text{ave}} \quad (7)$$

$$P = \pi\bar{\sigma}\ (2Ra - a^2)\ln\left(\frac{2R}{2R - a}\right) \quad (8)$$

Therefore, the material flow stress is:

$$\bar{s} = \frac{P}{p(2Ra - a^2)\ln(2R/(2R - a))} \quad (9)$$

And the relationship between flow stress ($\bar{\sigma}$) and axial average stress, i.e. $(\sigma_z)_{ave}$ is as following:

$$\bar{\sigma} = (\sigma_z)_{ave}[(1 - \frac{2R}{a})\ln(1 - \frac{a}{2R})]^{-1} \quad (10)$$

The above equation can be represented as follows:

$$\bar{\sigma} = (\sigma_z)_{\text{ave}}\,\acute{C}\ , \qquad \acute{C} = \left[\left(1 - \frac{2R}{a}\right)1n(1 - \frac{a}{2R})\right]^{-1}) \quad (11)$$

$$R = \frac{h^2 + (d_2 - d_1)^2}{4(d_2 - d_1)} \quad (12)$$

Where, C' is called bending correction factor. The value of R is the radius of curvature of the barreled sample. This radius can be obtained based on the size of the different parts of the barreled sample. For this purpose, the following formula is used:

The Method of Numerical Correction Factor

The method of numerical correction factor is performed with finite element simulation of pressure test using stress-strain curve obtained from a bending correction factor in the first step of the simulation. Then by measuring the height of the sample in several stages, in order to calculate the equivalent strain and measuring the diameter of the middle-level of the simulated sample like pressure test, by dividing the force resulted from simulation by the middle section area of the segment, the average strain is calculated. By dividing the average stress obtained from stress-strain curve in each equivalent strain, the numbers obtained from this division are multiplied by the experimental average stress-strain curve. The re-simulation of this experiment using the obtained stress-strain curve, the above steps is repeated (Saniei and Fatehi, 2006).

To investigate the effect of strain rate in tests, all tests were conducted at the same average strain rate and velocity at each stage is calculated as follows:

$$\dot{\varepsilon} = \frac{\varepsilon}{t}, \varepsilon = \ln(\frac{h_0}{h}) \quad (13)$$

$$v = \frac{h_0 - h}{t} \quad (14)$$

Where, v is the velocity, $h_0$isthe initial height of sample and h is the height of the sample after each stage of testing. By combining the relations of strain and strain rate and eliminating t from relations, for the velocity of performing the experiment, the final equation is obtained as follows:

Description Pressure Test

Pressure test has been used to determine the flow curve for AZ60alloy.In performing the tests carried out, the following points have been considered:

1. In each experiment, the sample has been kept for five minutes at the desired temperature.
2. The experiments were performed without lubrication.
3. The dimensional ratio of the sample has been based on the ASTM standard (height to diameter ratio equal to 1.5).
4. The strain rate at the pressure test has been kept constant.

All samples have a nominal diameter of 6mm and height of 9mm. Samples were prepared by machining. The experiments were performed by SANTAM 150kN apparatus. In this device the upper jaw is adjustable. To perform pressure test, at least 8 identical cylindrical specimens were turned for each curve and then each cylinder was compressed up to a certain amount at one stage, the results related to force and geometrical deformations of the sample were measured and recorded. In order to determine the effect of strain rate in experiments, all tests were conducted at the same average rate of strain.

The Characteristics of Samples and Templates

AZ 60 magnesium alloy was prepared as cast. The cylindrical specimens with diameter of 6mm and length of 9mm were prepared by machining. For the experimental study of the effect of the radius of the corners of templates, a distinct template with a corner radius of 1mm was provided. To make the template, steel 1.2713 according to DIN standards was used. Each frame consists of two parts; the first part is cylindrical with radius of 29mm that a V-shaped groove was created in it by wire cutter device. The other part is cylindrical that its inside has been machined as much as the first part such that the first part can be completely included in the second part. Geometrical characteristics of the template have been shown in figure 1.To investigate the effects of temperature, lubrication and friction conditions, and the radius of corners of the template of empirical experiment is shown in Table 2. Furthermore, some experiments were carried out at two temperatures of 230 and 250°C and at strain rates of $0.01s^{-1}$on AZ 60 alloy and in conditions without lubricant.

Table 1: Magnesium alloy composition

Material	Mg	Al	Zn	Mn
AZ60	Bal.	9.5	0.5	0.3

Table 2: Specifications of experiments carried out

Material	Temperature	Velocity(mm/min)	Fillet radius(mm)	Lubricant
60AZ	230	1	1	MoS2 & Dry
60AZ	250	1	1	MoS2 & Dry

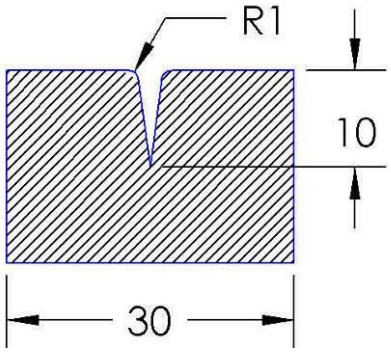

Figure 1: Geometrical properties of the test templates

The Mechanical Properties of the Alloys

Mechanical properties and stress-strain behavior of the used AZ 60magnesium were obtained using simple pressure tests. These stress-strain curves were obtained at 230 and 250°C and velocity of 1mm/min. Also at two temperatures of 230 and 250°C and at strain rates of 0.001, 0.01 and 0.1s^{-1}, the tests was performed on AZ60 alloy, and the results of the pressure tests have been used. Also, the bending correction factor and the numerical correction factor have been used to eliminate the frictional effect between surfaces in test results. In fact, the corrected results have been used in simulation. Experiments have been conducted by SANTAM 150kN.The obtained stress-strain curves are shown in Figure 3.It is known that AZ 60 magnesium alloy has softness strain behavior. To obtain better results in the finite element simulation, each curve has been introduced as an input to the software.

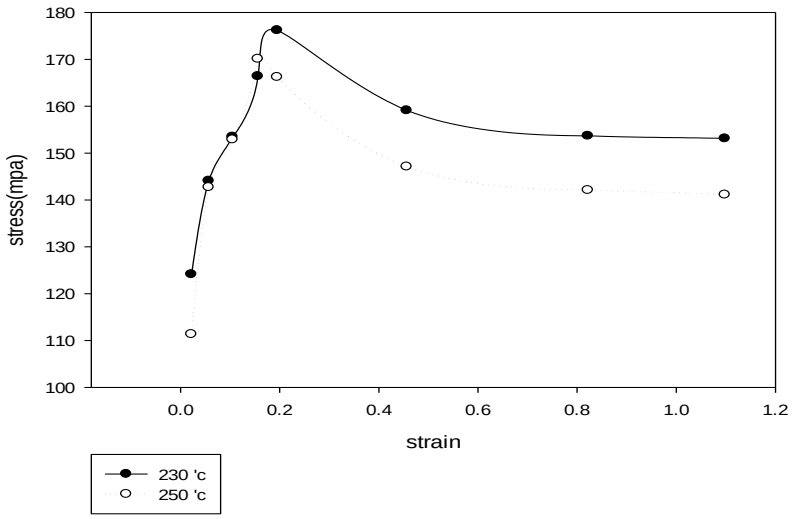

Figure 3: Stress-strain curve of AZ 60 magnesium alloy

The Parameters used to Measure the Effect of Friction

The sensitivity of the slope is defined as follows:

$$\lambda_k = \frac{K_m - K_{m=MoS2}}{K_{m=MoS2}} \qquad (16)$$

Where, K_m is the slope of force curve with friction factor of *m* and $K_{m=MoS2}$ is the slope of the force curve at conditions that the lubricantMoS2 is used. To calculate the slope of the curve, according to Figure 4, the slope of the linear part of the force curve has been used. Sensitivity to the length of the extruded section can be defined as follows:

$$\lambda_H = \frac{H_m - H_{m=MoS2}}{H_{m=MoS2}} \quad (17)$$

Where, H_m is the slope of force curve with friction factor of *m* and $H_{m=MoS2}$ is the slope of the force curve at conditions that the lubricant MoS2 is used.

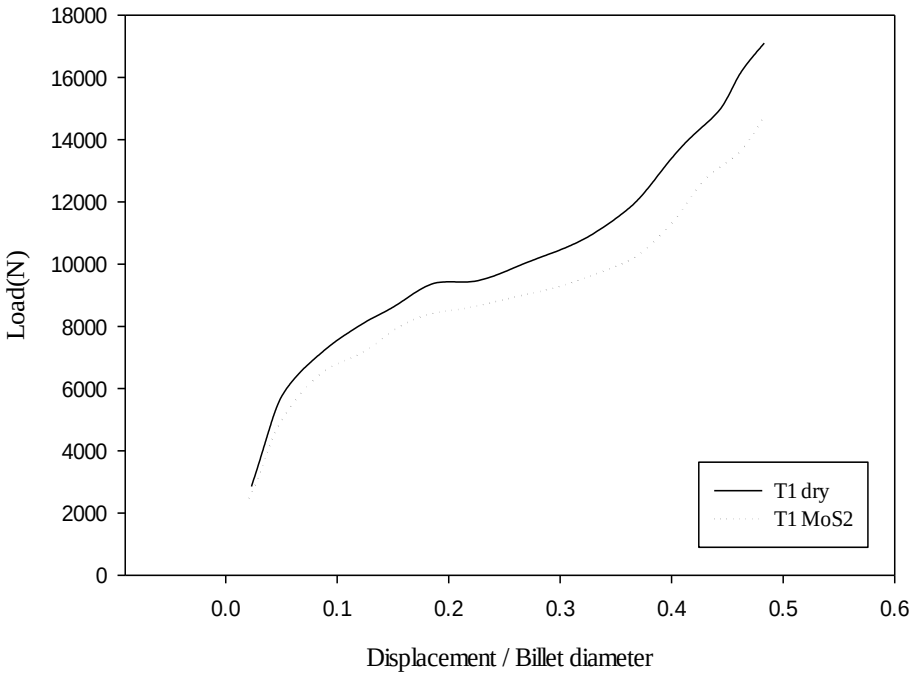

Figure 4: Experimental force-displacement curve of AZ 60 magnesium alloyat temperature of 230°C

RESULTS AND DISCUSSION

Results and Analyses

Results of AZ60 Alloy Pressure Tests

The pressure tests of AZ60 magnesium alloy were done at temperatures of 230 and 250°C and under the loading of $0.001s^{-1}$, $0.01s^{-1}$, and$0.1s^{-1}$. After each experiment, the samples were rapidly cooled within chilled water. Then, the upper, middle, and lower diameters of the barreled specimen were measured. The mean upper and lower diameters have been used in calculating bending radius. Then, based on the data for each curve, the radius of the middle section (a) was obtained. The equations (11) and (12) were used to obtain the radius of bending(R) and bending correction factor respectively. Initial stress value is obtained from bending correction factor, and then by using finite element simulation and DEFORM 2D software and multi-stage correction, correction factors for each temperature and certain strain rate have been obtained. Figure 5 shows the different stages of deformation in the simulated sample at temperature of 250°C and strain rate of $0.001s^{-1}$. At each simulation, the behavior of the material as a function of temperature and strain rate and as a table has been introduced to the finite element DEFORM 2D software.

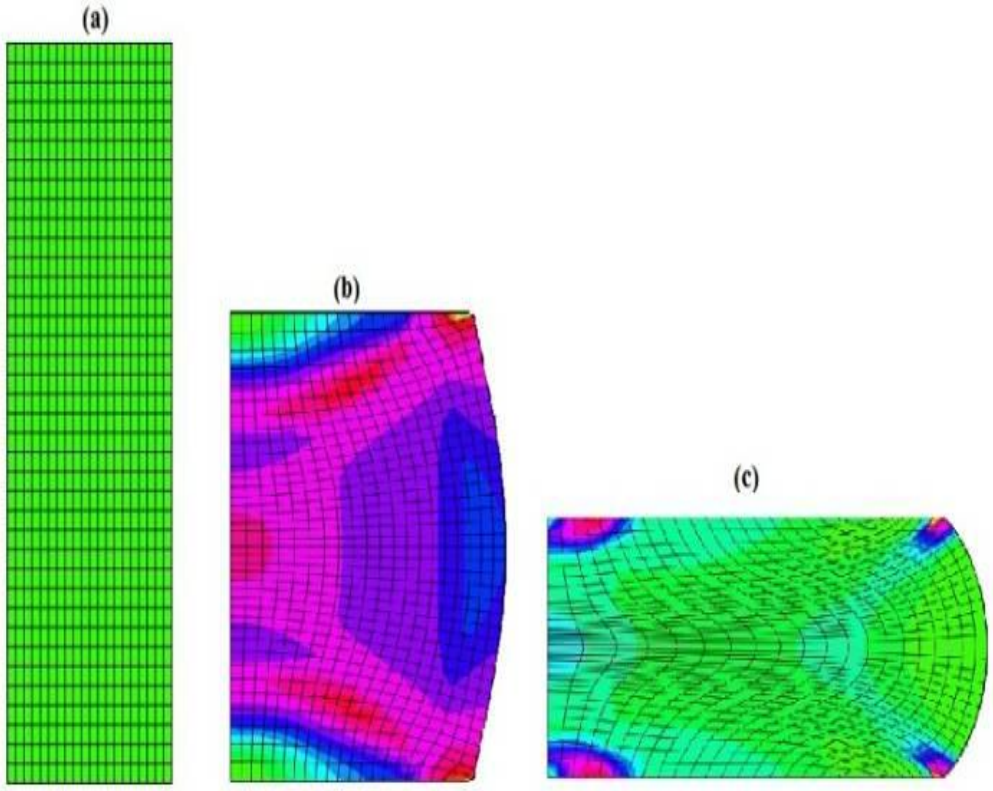

Figure 5: Various stages of deformation of simulated sample: (a) prototype (b) after the 3mm of deformation (c) after the 6mm of deformation

The results obtained in Tables 3 to 5 for temperature of 230°C and strain rates of $0.001s^{-1}$, $0.01s^{-1}$ and $0.1s^{-1}$have been provided. It is clear that in the small strains, both correction factors are approximately the same, but with increasing the strain, the differences become greater and the numerical correction factor has desired results.

Table 3: Results of the pressure test for AZ60alloy at temperature of 230°C and strain rate of $0.001s^{-1}$

No.	Force (N)	Final height (mm)	Final Mid Radius (mm)	R (mm)	BCF	NCF
1	2756.18	8.8	3.07	336.98	1.002	1
2	3765.89	8.5	3.10	270.75	1.003	1
3	4419.00	8.1	3.14	168.44	1.005	1
4	4991.12	7.7	3.27	122.04	1.009	1.0001
5	5500.75	7.4	3.36	66.96	1.013	1.002
6	5821.52	5.7	3.79	10.31	1.081	1.008
7	6936.83	3.8	4.42	12.99	1.099	1.034
8	8533.27	3.0	4.78	10.13	1.147	0.989

Table 4: Results of the pressure test for AZ60 alloy at temperature of 230°C and strain rate of 0.01s^{-1}

No.	Force (N)	Final height (mm)	Final Mid Radius (mm)	R (mm)	BCF	NCF
1	3847.46	8.8	3.12	293.14	1.003	1
2	4480.38	8.5	3.16	226.48	1.003	1.001
3	4972.86	8.1	3.20	182.27	1.004	1.001
4	5513.60	7.7	3.25	128.86	1.006	1.002
5	6159.78	7.4	3.35	58.69	1.015	1.005
6	6833.13	5.7	3.72	25.33	1.039	1.009
7	86007.30	3.8	4.41	13.36	1.095	1.039
8	9444.22	3.0	4.51	9.96	1.139	0.98

Table 5: Results of the pressure test for AZ60alloy at temperature of 230°C and strain rate of 0. 1s^{-1}

No.	Force (N)	Final height (mm)	Final Mid Radius (mm)	R (mm)	BCF	NCF
1	3953.00	8.8	3.07	354.34	1.002	1
2	4855.78	8.5	3.08	184.89	1.004	1
3	5584.73	8.1	3.18	175.33	1.005	1.001
4	6097.95	7.7	3.26	77.16	1.011	1.002
5	6695.54	7.4	3.36	56.11	1.015	1.006
6	7817.05	5.7	3.69	25.16	1.039	1.015
7	8938.09	3.8	4.21	12.73	1.096	1.042
8	12115.26	3.0	4.85	10.96	1.136	1.001

Based on the results obtained, the stress-strain curves of AZ60 alloy have been extracted. In Figure 6, the curves of pressure test with bending correction factor and numerical correction factor have been drawn. At low strains, the rate of stress calculated from numerical correction factor and bending correction factor slightly vary. But by increasing strain, the difference of stress calculated from numerical correction factor and that of bending correction factor becomes grater, and always the stress calculated from bending correction factor is higher. Magnesium alloys generally have fixed behavior at elevated temperature and under pressure. After working, the initial hardness reaches maximum point, and the material suffers from softness strain and its flow stress reduces. This softness strain is the result from changes in structure of these alloys, temperature effects, and the velocity of loading in their structures, especially dynamic re-crystallization effect which is explained by increasing the saved thermal activating energy, and changing the microstructures during the process of elevated temperature pressure test. Finally, the material has a stable behavior. In figure (7), the comparison between displacement-force curves obtained from the correction factors has shown.

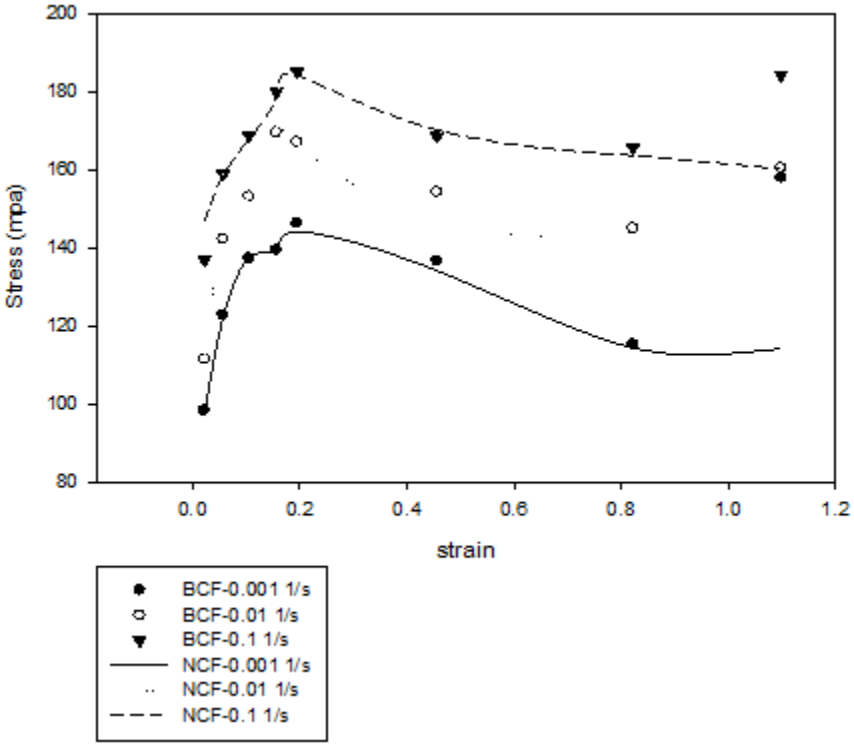

Figure 6: The results of pressure tests of AZ60 alloy at temperature of 250ºC and different strain rates

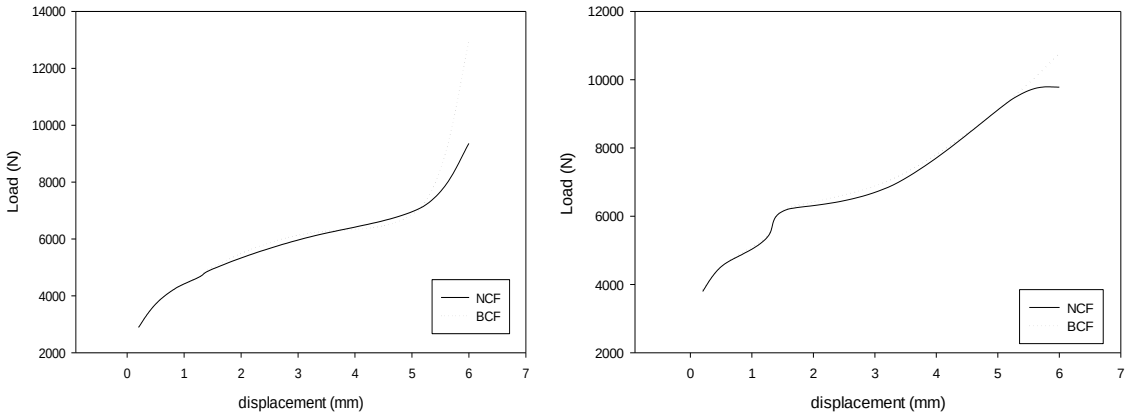

Figure 7: The comparison between displacement-force curves for AZ60 alloy obtained from the correction factors: (a) at temperature of 230ºC and strain rate of 0.01s^{-1}, (b) at temperature of 250ºC and strain rate of 0.01s^{-1}

The Effect of Temperature and Strain Rate in Correction Factor

Strain rate and temperature are effective in material flow stress, the rate of hardening and softness strain. Figure 8 shows the effect of strain rate in numerical correction factor at temperature of 250ºC.At each temperature, by increasing strain rate; the numerical correction factor does not significantly change at low strains. But, by increasing strain rate, the value of numerical correction factor increases and at lower strains, it reaches its maximum value. In other words, at intermediate strains, by increasing strain rate, the value of correction factor decreases. But at high strain, such that it was predicted, the numeral correction

factor is decreased that the reason of this is the increasing of friction effect in forming force. However, at high strains, the reduction rate of numeral correction factor decreases with increasing the strain rate. In fact, by increasing strain rate the rate of friction and its effect in forming force and deformation of the sample has reduced.

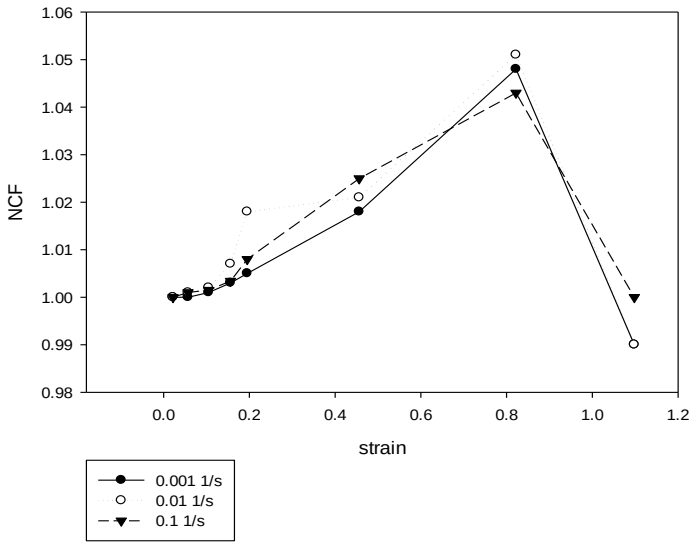

Figure 8: The effect of strain rate in numerical correction factor in pressure test of AZ60 alloy at temperature of 250ºC

Figure 9 shows the effect of strain rate in bending correction factor (BCF) at temperature of 250ºC. At a fixed temperature, by increasing strain rate, the bending correction factor does not significantly change at low strains. But, by increasing strain rate, the value of bending correction factor always increases. The reason for this fact is the ignoring of internal friction effect in forming forces related to BCF. In fact in this method, only the effect of geometry is considered. The strain rate and temperature are effective in friction. In numerical simulations, these effects are considered and the results are close to reality.

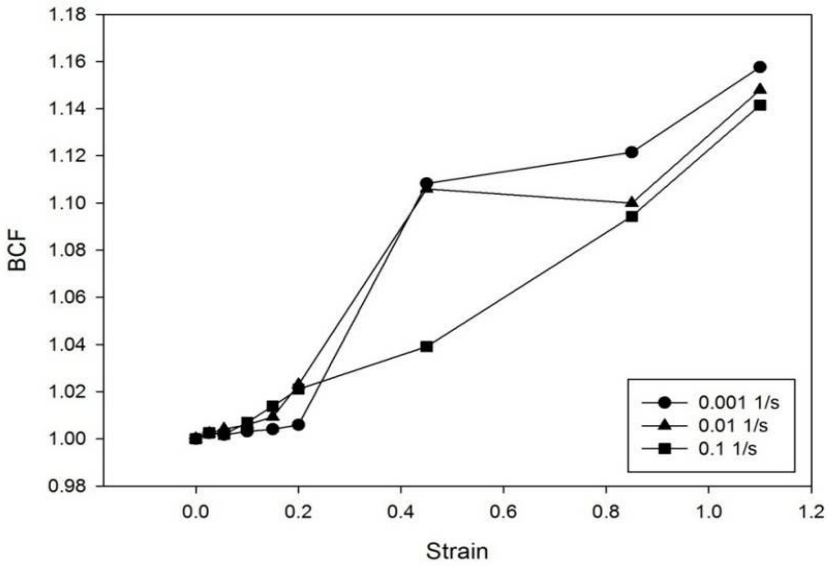

Figure 9: The effect of strain rate in bending correction factor in pressure test of AZ60 alloy at temperature of 250ºC

The effect of temperature on the numeral correction factor has been shown in figures 10 to 12. In low strains, intelligible changes are not seen in numeral correction factor, but by increasing the strain, the effect of temperature becomes clear. In intermediate strains, the difference of the values of numeral correction factor increases and at more elevated temperatures, higher values of numerical correction factor are required. As mentioned previously, the value of bending correction factor always increases and at high strains, it creates more errors. Therefore, at high strains, the stress corrected by this method is significantly different from actual stress, and then the predicted forming force by this method is more than actual force obtained in pressure test and the necessity of using numerical correction factor and considering all actual conditions of pressure test is completely obvious. In higher strain rates, the effect of temperature in numerical correction factor is higher and more sensible. The reason of this phenomenon is the increasing of friction effect on temperature and higher strain rate.

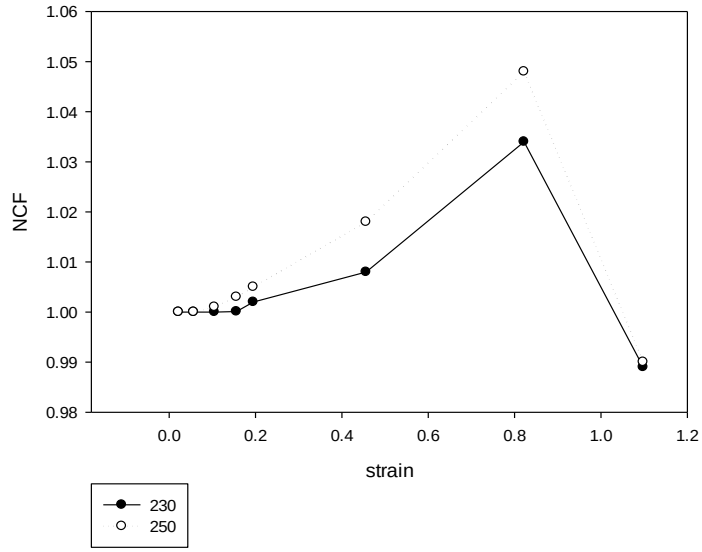

Figure 10: The effect of temperature in numerical correction factor in compression test of AZ60 alloy at strain rate of 0.001s^{-1}

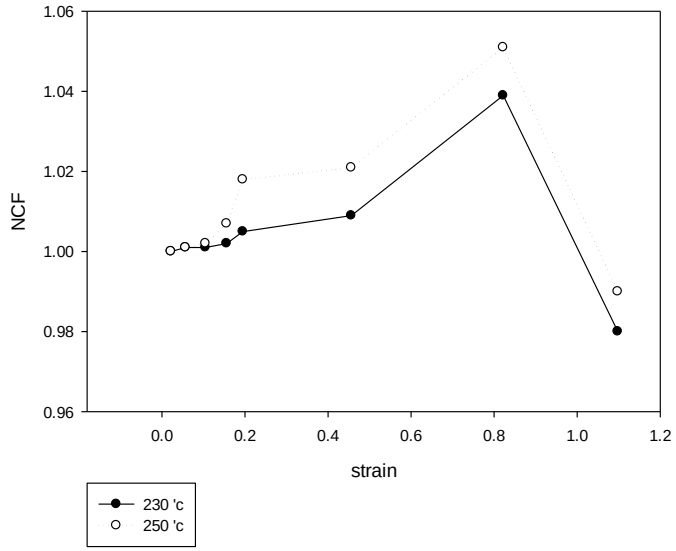

Figure 11: The effect of temperature in numerical correction factor in compression test of AZ60 alloy at strain rate of 0.01s^{-1}

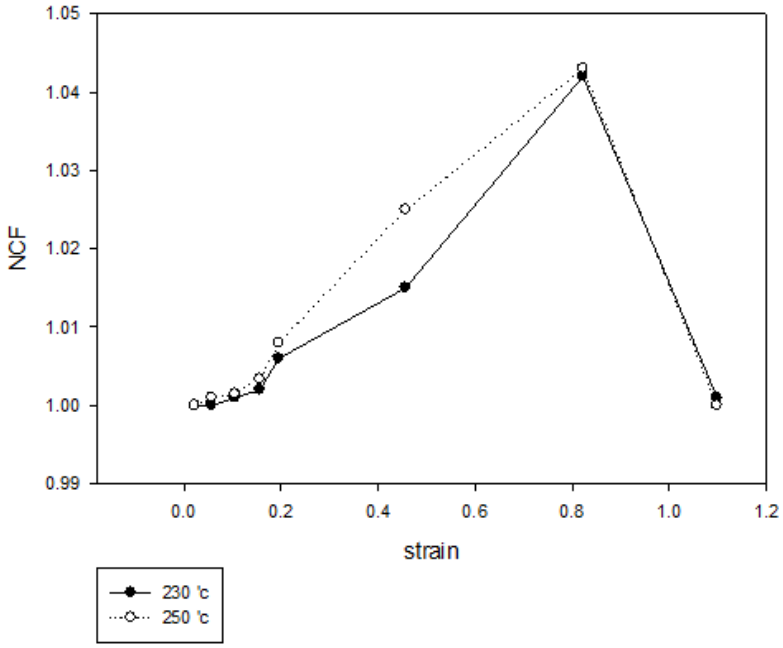

Figure 12: The effect of temperature in numerical correction factor in compression test of AZ60 alloy at strain rate of 0. 1s^{-1}

In figures 13 to 15, the effect of temperature on the bending correction factor has been shown. According to above figures, at a fixed strain, by increasing the temperature, the higher value of correction factor has been obtained. However, the value of bending correction factor has been continuously increased in all temperatures by increasing the strain rate. At higher temperatures, the rate of changes of numerical correction factor was higher proportion to 1 (stress state without needing correction). In fact, in intermediate strains, by increasing temperature, the numeral correction factor has become larger. The value of friction factor in forming magnesium alloys always depends on strain rate and forming temperature. Bending correction factor is fully geometrical and the effect of other parameters of the process is not considered. Hence, by varying the temperature and strain rate, the amount of created error in bending correction factor still exists. But since the numerical correction factor considers the effect of actual parameters of shaping, by changing the temperature and strain rate, the obtained answers from numerical correction factor are more consistent with the results of experimental tests.

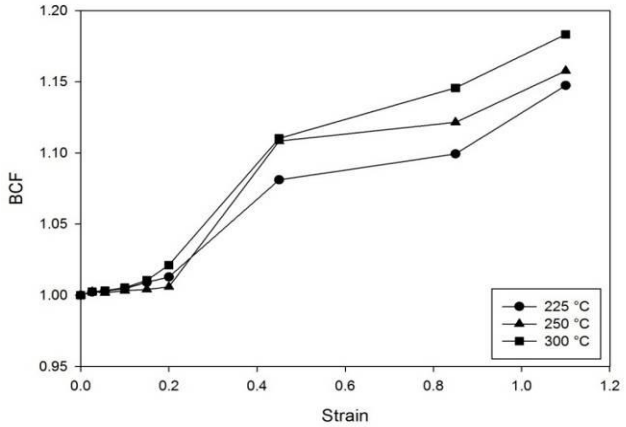

Figure 13: The effect of temperature in bending correction factor in compression test of AZ60 alloy at strain rate of 0.001s^{-1}

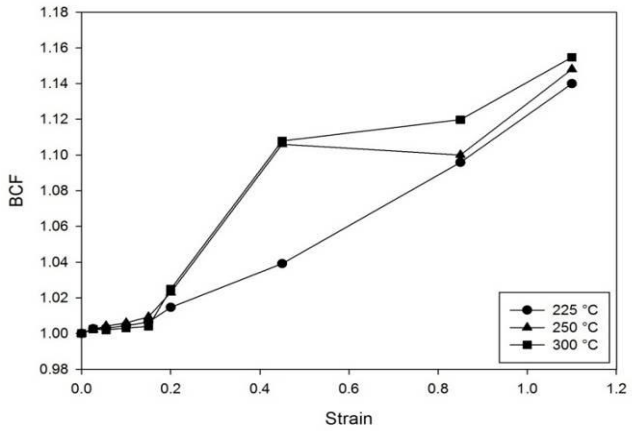

Figure 14: The effect of temperature in bending correction factor in compression test of AZ60 alloy at strain rate of 0.01s^{-1}

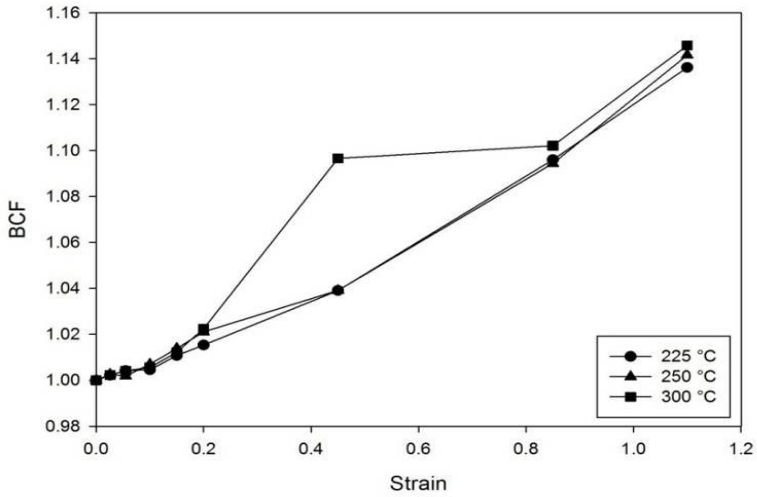

Figure 15: The effect of temperature in bending correction factor in compression test of AZ60 alloy at strain rate of 0. 1s^{-1}

Conclusion

In this paper, by doing pressure tests on AZ41 magnesium alloy, stress-strain behavior of these alloys at high temperatures and different velocities of deformation have been studied. Since the frictional behavior of a material in production processes especially forming processes is used, the frictional behavior of this alloy in different temperatures of deformation has been analyzed. T-shape pressure test that is considered as a test to measure friction and has a close affinity with real conditions of forming processes such as forging and extrusion has been studied. Compression tests of AZ60 magnesium alloy at temperatures of 230 and 250°C and under the loading rates of 0.001s^{-1},0.01s^{-1}, and 0.1s^{-1}have been performed. After performing each test, the samples have been rapidly cooled in chilled water. The initial value of stress has been calculated with bending correction factor and then by finite element simulation with DEFORM software and multistage correction, the numerical correction factors for each temperature and fixed strain rate were obtained. At each simulation, the behavior of the material as a function of temperature and strain rate and in the form of tables is presented that the following results were obtained:

1. The bending correction factor always increases with increasing strain, while the numerical correction factor reduces in high strains and by increasing the effect of friction in the process.
2. In stress-strain curves of AZ60 alloy in low strains stress, the values of stress calculated from numerical correction factor and bending correction factor have very little difference; but by increasing the

strain, the difference of stress calculated from numerical correction factor and that of bending correction factor becomes more and always the calculated stress is higher than bending correction factor.
3. The total changes in the correction factors at all cases are the same, and do not depend to type of material. In other words, in AZ60 alloy, bending correction factor increases with increasing strain; and in high strains, the numerical correction factor decreases after increasing.
4. At a specified temperature, with increasing the strain rate, at low strains, the value of bending correction factor is not significantly different; but with increasing strain, the value of bending correction factor always increases.
5. Bending correction factor at all temperatures has continuously increased with increasing strain.
6. In compression test, the material maximum stress is sensitive to strain rate and forming temperature. At a constant temperature, with increasing strain rate, the material maximum stress increases and at fixed strain rate with increasing temperature, the maximum stress reduces.

REFERENCES

Abedi HR, Zarei-Hanzaki A, Fatemi-Varzaneh SM and Roostaei AA (2010). The semi-solid tensile deformation behavior of wrought AZ31 magnesium alloy. *Materials & Design* **31** 4386–4391.
Aghayani M and Khosro Niroumand B (2011). Effect of ultrasonic treatment on microstructure and tensile strength of AZ41 magnesium alloy.
Anbuselvan S and Ramanathan S (2010). Hot deformation and processing maps of extruded ZE41A magnesium alloy. *Materials & Design* **31** 2319–2323.
Cáceres CH (2009). Transient environmental effects of light alloy substitutions in transport vehicles. *Materials & Design* **30** 2813–2822.
Caton PD (2002). Magnesium — an old material with new applications. *Materials & Design* **12** 309-316.
Chen Qiang, Zhao Zhixiang, Shu Dayu and Zhao Zude (2011). Microstructure and mechanical properties of AZ41D magnesium alloy prepared by compound extrusion.
Ebrahimi R, Zahiri SH and Najafizade A (2006). Mathematical modeling of the stress–strain curves of Ti-IF steel at high temperature. *Journal of Materials Processing Technology* **171** 301–305.
Ettouney OM and Hardt DE (1983). A Method for In-Process Failure Prediction in Cold Upset Forging. *ASME Journal of Engineering for Industry* **105** 161–167.
Ettouney OM and Stelson KA (1990). An Approximate Model to Calculate Foldover and Strains during Cold Upsetting of Cylinders Part 1: Formulation and Evaluation of the Foldover Model. *ASME Journal of Engineering for Industry* **112** 260–266.
Fereshteh Saniee F, Fallah Nejad Kh, Beheshtiha A Sh and Badnava H (2013). Investigation of tension and compression behavior of AZ80 magnesium alloy.
Fereshteh-Saniee F, Barati F, Badnava H and Fallah-Nejad Kh (2012). An exponential material model for prediction of the flow curves of several AZ series magnesium alloys in tension and compression.
He X, Yu Z, Liu G, Wang W and Lai X (2010). Mathematical modeling for high temperature flow behavior of as-castTi–45Al–8.5Nb–(W, B, Y) alloy. *Materials & Design* **30** 166–169.
Kim WJ, Lee MJ, Lee BH and Park YB (2010). A strategy for creating ultrafine-grained microstructure in magnesium alloy sheets.
Li Caixia and Yu Yan-Dong (2013). The effect of solution heat treatments on microstructure and hardness of ZK60 magnesium alloys prepared under low-frequency alternating magnetic fields.
Liao Haoming, Tang Guoyi, Jiang Yanbin, Xu Qing, Sun Shiding and Liu Jianan (2011). Effect of thermo-electropulsing rolling on mechanical properties and microstructure of AZ31 magnesium alloy.
Masoudpanah SM, Mahmudi R and Roostaei AA (2010). The microstructure, tensile, and shear deformation behavior of an AZ31 magnesium alloy after extrusion and equal channel angular pressing. *Materials & Design* **31** 3512–3517.
Mathis K, Trojonava Z and Lukac P (2002). Hardening and softening in deformed magnesium alloys. *Materials Science and Engineering: A* **324** 141–144.

Mielnik EM (1991). *Metalworking Science and Engineering* (McGraw Hill International Book Company).
Narayanasamy R, Sathiyanarayanan S and Ponalagusamy R (2000). A study on barreling in magnesium alloy solid cylinders during cold upset forming. *Journal of Materials Processing Technology* **101** 64-69.
Palumbo G, Sorgente D and Tricarico L (2010). A numerical and experimental investigation of AZ31 formability at elevated temperatures using a constant strain rate test. *Materials & Design* **31** 1308–1316.
Saniee F and Fatehi-Sichani F (2006). An investigation on determination of flow curves at room temperature and under forming conditions. *Journal of Materials Processing Technology* **177** 478–482.
Shuyan Wu, Zesheng Ji and Tielei Zhang (2009). Microstructure and mechanical properties of AZ31B magnesium alloy recycled by solid-state process from different size chips.
Wang Ya, Zhou Ji,Wang Jie, Luo Tian and Yang Yuan-sheng (2011). Effect of Bi addition on microstructures and mechanical properties of AZ80 magnesium alloy.
Zhao Z, Chen Q, Chao H and Huang S (2010). Microstructural evolution and tensile mechanical properties of thixoforged ZK60-Y magnesium alloys produced by two different routes. *Materials & Design* **31** 1906–1916.
Zhou HT, Li QB, Zhao ZK, Liu ZC, Wen SF and Wang QD (2010). Hot workability characteristics of magnesium alloy AZ80, A study using processing map. *Materials Science and Engineering: A* **527** 2022–2026.